

# MELT-CONCRETE INTERFACE HEAT TRANSFER MODELS AND COOLABILITY MODELS: PWR ANALYSES WITH MELCOR/CORCON AND CORQUENCH

**A. Rýdl, B. Jäckel**

Laboratory for Thermalhydraulics, Paul Scherrer Institut  
5232 Villigen, Switzerland  
adolf.rydl@psi.ch; bernd.jaeckel@psi.ch

**J-U. Klügel and P. Steiner**

Kernkraftwerk Gösgen-Däniken AG  
4658 Däniken, Switzerland  
jkluegel@kkg.ch; psteiner@kkg.ch

## ABSTRACT

The MELCOR and CORQUENCH codes are used for simulations of the late phase of a postulated total SBO at KWU KONVOI PWR reactor. The base line SBO sequence without any mitigation and some of its variants are simulated in detail with MELCOR, selected cases up to 10 days of the accident progression. The ex-vessel phases of these scenarios, with long-term molten core-concrete interactions (MCCI), are recalculated also with the specialized code CORQUENCH. The AM counter measures after the reactor pressure vessel failure, typically flooding of the melt by water from the top at different times, are taken into account. The incentive for the work was to investigate the retention of corium materials, which were subject to MCCI, for this particular type of containment. At the same time, the detailed analysis is performed of the effect of different models employed for the description of heat transfer at the melt-concrete interface (ablation modeling) and of the effect of the “coolability” models. The results of the calculations indicate that this type of the KONVOI containment is relatively resistant to challenges by the late-phase accident progression. The incorporation of the CORQUENCH coolability models into MELCOR/CORCON, where it is missing, should be of primary interest. The model of the heat conduction into concrete behind the ablation front could also be useful. The overall impact of this modeling option -which is available in CORQUENCH and not available in MELCOR- on the maximum ablation depth seems to be relatively high under conditions pertaining to our accident simulations.

## KEYWORDS

MCCI, heat transfer models, coolability models, CORQUENCH, MELCOR

## 1. INTRODUCTION

The late phase of a postulated severe accident in case of reactor pressure vessel (RPV) failure is characterized by the interactions of molten materials from the reactor with the concrete basemat of the containment. These interactions, molten core-concrete interactions (MCCI), are mostly driven by the decay heat within the melt. With melt temperatures above the decomposition temperature of a given concrete the basemat and other structures of the containment can be compromised due to significant erosion of the concrete by the melt. That is, the integrity of the last barrier preventing the release of fission products, FP, to the environment is threatened. The ability to predict the rate of the concrete decomposition and the amount of non-condensable gases generated from MCCI is crucial for assessing

the timing and the mode of the potential containment failure. Another important aspect of the MCCI studies is the "coolability" of the melt, i.e. the possibility to quench the melt in cavity, typically by adding water atop the melt as a part of late-phase accident management (AM), with far-reaching practical consequences.

MCCI in general and coolability of the melt in particular have been studied in many international research programs in the past 30 years (e.g., MACE and OECD-MCCI 1 and 2 [1], VULCANO [2], BETA [3]). Also, based on the experimental results, several specialized computer codes have been developed for simulations of the MCCI evolution and for coolability predictions. The computational tools used for the analyses in this work are MELCOR 1.8.6 [4] and the specialized code CORQUENCH [5] for the simulations of quenching behaviour of the flooded melt in cavity, developed in Argonne National Labs. The MELCOR code of the US NRC is established in Switzerland as the primary tool for integral severe accident analysis. The MCCI evaluations in MELCOR are driven by CORCON-Mod3 [6], which was formerly a stand-alone code, but is today fully integrated in MELCOR.

The MELCOR/CORCON code and the CORQUENCH code are used for simulations of MCCI in a postulated long-term total SBO scenario at the 1000MWe KWU KONVOI PWR of the type operated at Gösigen, Switzerland (Kernkraftwerk Gösigen, KKG). The objective is to investigate the response of the KKG cavity to long-term MCCI, in terms of the cavity concrete ablation, given the successful implementation of counter AM measures. The chief concern is the basemat melt-through, the depth of the axial (downward) concrete ablation, together with the potential for quenching of the melt which would stop the MCCI progression completely. In comparison to other similar studies we do not address the containment overpressurization by non-condensable gases from concrete decomposition since the KKG containment is protected with the Filtered Containment Venting System (FCVS). Also, the erosion of the concrete in the radial direction (sideways) is not considered to be of major importance for this particular type of containment. Complete spreading of the melt early after vessel failure is assumed in what is originally a relatively narrow space in this type of cavity. In line with the default MELCOR approach, the homogeneous melt configuration is assumed to form in the containment cavity after vessel failure in all calculations, i.e., the melt is not stratified.

As a part of the current work, the effect of different MCCI heat transfer models used in MELCOR/CORCON and CORQUENCH is analyzed in the integral simulations, the detailed description of the models themselves is given in chapter 2. As shown in previous studies ([7], [8]) the missing coolability models render MELCOR/CORCON incapable of assessing the potential quenching of the melt when water is present atop the melt. Hence, the specialized code CORQUENCH is used for analysis of cases where after vessel failure (VF) water could be delivered to cavity. The overview of the coolability models is given in chapter 3. The base case selected for our KKG MCCI simulations was the SBO scenario without manual reactor coolant system (RCS) depressurization and without any induced RCS failures before VF. Chapter 4 describes the MELCOR/CORCON and CORQUENCH analyses of the base case sequence and its variants. The sequences are calculated up to 10 days of MCCI after vessel failure. In chapter 5, the coolability of the melt in KKG cavity is assessed using the CORQUENCH code: First for the base case scenario trying to capture every detail of the late phase accident progression as predicted by MELCOR and then sensitivity analyses to cover a broader spectrum of scenarios where water could be delivered into the cavity and kept atop the melt for a long time as a part of long-term accident management. The overall results of the MELCOR and CORQUENCH analyses are summarized in chapter 6 and conclusions for the KKG cavity response to long-lasting MCCI are drawn.

## **2. HEAT TRANSFER FROM THE MELT TO CONCRETE**

As a first, rough approximation, the heat transfer in the molten pool from the pool to the horizontal and vertical surfaces of the concrete cavity is described as being governed by natural convection driven by

volumetric heating, the decay heat. This applies primarily to analyses where the concrete has low content of equivalent gases (CO<sub>2</sub> and steam which are released at concrete decomposition), i.e. mostly to analyses with siliceous concretes. If the equivalent gas content in the concrete is high, as it is in limestone concretes (LCS), the evolving gases will enhance the heat transfer and different heat transfer models would apply.

For the natural convection in volumetrically heated pools the heat transfer coefficient (or corresponding Nusselt number,  $Nu$ ) to a given surface is, in general, calculated from

$$Nu_x \sim Ra'^{\gamma} \quad (1)$$

where  $Ra'$  is internal Rayleigh number and  $\gamma$  is the experimentally determined constant. The subscript  $x$  remind us that  $Nu$ , and that is also the heat transfer coefficient, is a function of position on the cavity wall (in the simplest manner: the natural convection heat transfer to bottom horizontal surface is distinctly lower than the heat transfer to vertical sidewall). This is the same correlation which is used for description of the heat transfer in the in-vessel melt pool analyses, in particular in the IVR applications (In-Vessel Retention [9]). Characteristic length scale of the problem is always the melt layer thickness. In MELCOR/CORCON-Mod3 this type of relation is used for cases with "sufficiently low gas velocities" [6]. Different values of constants, multiplicative constant and constant  $\gamma$ , are used for vertical and horizontal cavity surfaces.

Otherwise, if the role of the gas bubbling is taken into consideration, the bubble-enhanced heat transfer is calculated based on the model devised by Kutateladze and Malenkov [10] when working with analogy between the developed nucleate boiling and the gas barbotage through a microporous plate into bulk liquid (the MCCI case for us). As adapted by Bradley [11], the primary correlation of the model can be cast in the form

$$Nu_A \sim \left( \frac{Pr p j_g}{g \mu} \right)^{2/3} \cdot f(\eta) \quad (2)$$

where  $Nu_A$  is based on a characteristic length equal to the Laplace constant,  $A = [\sigma/(g(\rho_l - \rho_g))]^{1/2}$ ,  $Pr$  is the Prandtl number for the liquid (molten pool),  $\rho_l$  and  $\rho_g$  are the densities of the liquid and the gas,  $\sigma$  is the liquid surface tension,  $\mu$  is the liquid viscosity,  $p$  is the pressure at the interface, and  $j_g$  is the superficial gas velocity (volumetric flow of the sparging gases). If  $j_g$  is higher than a certain threshold velocity,  $V_{tr}$  (where dimensionless  $\eta = j_g/V_{tr}$ ),  $Nu_A$  will be also a function of  $\eta$ , if  $j_g$  is below the threshold then  $f(\eta) = 1$ . This reflects the abrupt change in the heat transfer at the sparging gas velocity higher than the threshold: for many fluids, the  $V_{tr}$  as calculated inside CORCON as a function of  $\sigma$  and  $\mu$ , would represent transition from the bubbly to churn-turbulent flow. A simple picture of the bubble-enhanced convection case would imply that the mixing by gases can make the heat transfer distribution more uniform than in the natural convection case (and then the heat going to the bottom horizontal surface in cavity could be the same as the heat going to the vertical sidewalls).

The model is coded in CORCON-Mod3 with the imposed limit of choosing the greater of the  $Nu$  numbers calculated for the bubble-enhanced convection and for natural convection [6]. Not knowing about the exact implementation in the code we can try to work out a numerical example based on our reactor calculations, similar to ones presented in chapter 4 but with siliceous concrete: At an early stage of MCCI, for ~1 m deep melt pool in a PWR cavity and the internal heating of approximately 1 MW per cubic meter of the melt, the estimated value of  $Ra'$  in our calculation was roughly  $5 \times 10^{12}$ . This could represent –say for the sideward heat transfer- a natural convection  $Nu$  of about 200, depending on the particular form of the correlation 1 (e.g.,  $Nu = 0.85 Ra'^{0.19}$  [9]). At the same time, the correlation 2 for the bubble-enhanced convection, with calculated  $j_g = 6.5$  cm/s (being here about ten times higher than the corresponding  $V_{tr}$ ), shows  $Nu_A \doteq 1.5$ , with the characteristic length  $A = 0.003$  m. Thus, in this

instance and for siliceous concrete, the estimated value of the Nusselt number is higher for the natural convection case, though the corresponding sideward heat transfer coefficient is higher with the bubble-enhanced convection correlation (~2 kW/m<sup>2</sup>.K versus ~ 0.8 kW/m<sup>2</sup>.K).

## **2.1. Heat Transfer across the Melt-Concrete Interface**

Description of the heat transfer at the interface itself, at the compound interface where corium interacts with concrete, is more complicated than that of the heat transfer from the bulk volume due to the complex structure of the interface. In principle, there are two models between which the user of the MELCOR code (and, similarly, of the CORQUENCH code<sup>1</sup>) can choose in the input: the gas\_film model and the slag\_film model. The CORQUENCH interface heat transfer is based on exactly the same models.

### **2.1.1. Gas film model**

Originally, in early CORCON-Mod2 it was assumed solely that the gases released from concrete decomposition would form a stable film between the melt pool and the concrete. In this so called gas film model, the heat transfer from a liquid pool across the interface to the melting surface underneath is described -for horizontal or nearly horizontal surfaces- using the concept of the Taylor-instability bubbling [12], with Nusselt number based on the estimated thickness of the thin gas film which blankets the surface and from which the bubbles are released into the pool. On vertical surfaces, a flowing gas film is assumed with both laminar and turbulent character of the film taken into consideration in the appropriate convective heat transfer correlations. The heat transfer by radiation across the gas film is also included. A smooth transition between the bubbling model (Taylor-instability bubbling from a horizontal plate) and the film-flow model is ensured. The crust can form at the melt-film interface. The thickness of the crust is determined by local energy balances and the heat transfer across the crust is conduction limited. The gas\_film model is still a default input option in MELCOR, both in MELCOR 1.8.6 and MELCOR 2.1 versions.

### **2.1.2. Slag film model**

For what might be a more realistic case, with not so high gas release at MCCI (typically with siliceous concretes), an alternative model has been devised by Bradley [11] in CORCON-Mod3. It is so called slag\_film model. It takes into account much of the complexity of the interface, usually represented by several distinct layers. There is an overheated well-mixed liquid, molten corium pool, possibly with solid or partially solid crust on its outer regions, a slag layer (layer of "molten concrete") and then the unablated concrete. Periodic growth and removal of slag from the interface may also lead, depending on the pool temperature, to periodic growth and removal of the crust [6], periodicity given by the growth of the evolving gas bubbles and their departure. Crust is thus permeable not only to gases but also to transfer of the concrete decomposition products from the interface to the bulk pool. At bubble departure, the buoyancy of the concrete slag in the denser molten core material helps to displace the slag from the surface [11].

A set of simplified energy equations describing simultaneous concrete melting and molten corium solidification during a bubble cycle is solved [13], subject to continuity of temperature at each interface and continuity of heat flux (including effects of phase change) at each interface. The system in question consists, generally, of four regions: the solid substrate (concrete), the layer of melting substrate (slag), molten phase and the solidified molten phase crust (crust calculated by CORCON has always the same composition as the molten pool). The energy equations are solved for the instantaneous interface

---

<sup>1</sup> in CORQUENCH, as a third option, one can also choose an empirical correlation developed by Sevón [5]

temperature,  $T_i$ , and the melting crust growth as a function of molten corium temperature,  $T_{pool}$ , the ablation temperature of the concrete,  $T_c$  and the thermophysical properties of the four regions.

From rather detailed numerical analyses of the predicted interfacial temperatures as functions of the pool temperatures for different pool compositions (mixed oxides or steel) surprisingly simple conclusion was drawn by Bradley [6]: Within the range of the expected uncertainties the heat transfer coefficient across the interface,  $h_{slag}$ , is a constant multiple of the heat transfer coefficient from the bulk pool to the interface,  $h_{pool}$ , irrespective of the pool composition and temperature:

$$h_{slag} = c_{slag} \cdot h_{pool} \quad (3)$$

where (constant)  $c_{slag}$  is defined by

$$c_{slag} = \frac{T_{pool} - T_i}{T_i - T_c} \quad (4)$$

with estimated value of 0.41 and  $h_{pool}$  is determined for natural convection from Eq. 1 or for bubble-enhanced convection from Kutateladze-Malenkov correlation in Eq. 2.

## 2.2. Application of Different Heat Transfer Models in Integral Simulations

The two individual heat transfer coefficients discussed in previous paragraphs, transfer from the bulk pool to interface and across the interface to concrete, represent convective heat resistances in series. The overall heat transfer coefficient,  $h_o$ , between the bulk molten pool and the concrete surface is thus given -say for the the slag\_film model on the interface- by

$$\frac{1}{h_o} = \frac{1}{h_{pool}} + \frac{1}{h_{slag}} \quad (5)$$

Substituting for  $h_{slag}$  from (3) into (5) results in

$$h_o = h_{pool} \left( \frac{c_{slag}}{c_{slag} + 1} \right) \quad (6)$$

and hence, for  $c_{slag} = 0.41$ ,

$$h_o = 0.29 h_{pool} \quad (7)$$

The resulting heat flux [W/m<sup>2</sup>] from the pool to concrete, either radially or axially, is then

$$q = h_o (T_{pool} - T_c) \quad (8)$$

In MELCOR, the slag\_film model (or, alternatively, the gas\_film model) can be chosen in input independently for axial and radial heat transfer calculations; perhaps only using the same option for both directions makes real sense. The coefficient  $h_{pool}$  is calculated by the code without a possibility of user intervention. The same applies to CORQUENCH. For our base line SBO calculation with MELCOR, the default MELCOR option, i.e. the gas\_film model, was used for both radial and axial heat transfer modeling. In section 4.1, comparison of this approach is made with both the gas\_film and the slag\_film model results as calculated by CORQUENCH.

In the CORQUENCH code the heat transfer modeling closely resembles that of CORCON-Mod3 only that the CORQUENCH models are, in general, much more elaborated. For the axial, downward heat transfer a transition from the gas\_film to slag\_film can be calculated as a user option based on a threshold minimum velocity of the sparging gases. The really essential enhancement in CORQUENCH is a possibility -with the slag film model option on- to follow the transient heat transfer by conduction into concrete behind the ablation front, so called "concrete dry-out model" [14]. With this model not all of the heat transferred to concrete is going to ablation. This is, otherwise, a standard way of treating the concrete ablation process: In MELCOR/CORCON and in many other MCCI models the concrete conductivity is deemed to be so low that the heat transfer by conduction to concrete is neglected and all the energy

deposited into concrete goes directly into ablation. However, some of the OECD-MCCI tests and also some VULCANO tests showed that the heat sink provided by the (cold) concrete is important, at least in terms of the early crust formation. Currently, the inclusion of the transient heat conduction is considered to be important in evaluating both the early and late phases of MCCI [5]. The integral effect of this modeling option will be assessed for the base line SBO scenario simulation in chapter 4, comparing CORQUENCH and MELCOR results.

The whole picture of the heat transfer at the melt-concrete interface could be more complicated if we think about the physico-chemical restraints for the multi-component, multi-phase material mixture in close vicinity to the interface (“material accumulation must be related to physico-chemistry even if a strong deviation from thermodynamic equilibrium may occur”) [15]. Another complication could be the apparent heterogeneity of the materials released from the concrete decomposition, different for different concretes, and thus the necessity to relate the heat transfer modeling to peculiarities of a given type of concrete [16]. None of those complexities are taken into account in CORCON or CORQUENCH.

### 3. HEAT TRANSFER UPWARDS, COOLABILITY MODELS AND CORQUENCH CODE

The main differences in modeling between the two codes, MELCOR/CORCON and CORQUENCH, for flooded cavity conditions are schematically represented in Fig. 1, taken from [1]. The crucial thing is that CORQUENCH can calculate the heat losses from the melt pool to the overlying water by various mechanisms through the *porous crust* while MELCOR sees the crust as a solid plate permeable only to gases. None of the experimentally observed cooling phenomena can be modelled with MELCOR, the heat transfer from the crusted melt pool upwards to water can only occur in MELCOR by conduction (conduction limited crust). The mechanisms which are responsible for major heat losses to overlying water and which are all modelled by CORQUENCH are: i) water ingress through the porous crust, ii) melt eruptions to the water, and iii) the cooling phenomena linked to the unstable crust behavior. More details will be given in section 5, where the sensitivity analyses involving these mechanisms are presented for KWU cavity response to MCCI. Very detailed account of the coolability phenomena and models and the CORQUENCH coolability analyses is presented in various papers by Farmer and by Robb, for example [1], [7] or [17].

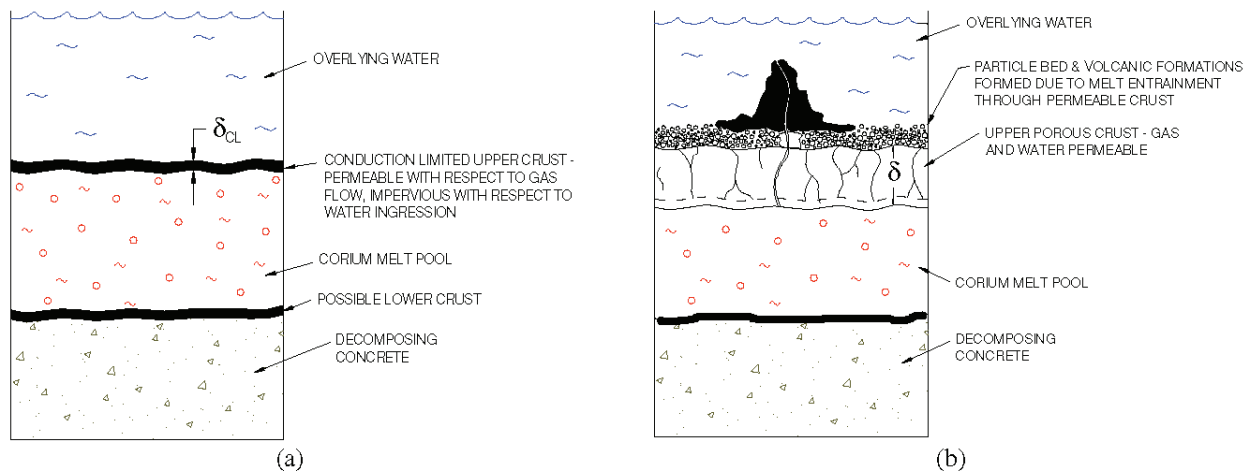


**Figure 1. Cooling mechanisms during MCCI in a) MELCOR/CORCON and b) CORQUENCH (Farmer et al., 2009 [1])**

For cases without water in cavity both MELCOR and CORQUENCH should yield similar results. Under such conditions, i.e. dry cavity, the heat transfer from the upper (crusted) surface is dominated by radiation to the structures above the debris pool. This is modelled in a similar way in both MELCOR and CORQUENCH. However, the upper crust in CORQUENCH can have a different material composition than the melt, can grow much thicker than the conduction limited crust in MELCOR, and can also contain a considerable fraction of the decay heat. All this may result in different predictions than MELCOR/CORCON would yield –see the calculations in the next chapter.

#### 4. BASE LINE SBO WITH MELCOR AND CORQUENCH

The simulations of the base case SBO sequence are described in this chapter. These analyses are mostly concerned with the MCCI phase of the sequences and, in particular, with the downward concrete erosion predicted by the codes in long term. The base line SBO is a sequence without any mitigation or operator intervention and without RCS depressurization. As modelled by MELCOR, the vessel failure is predicted at approximately 4.5 h. Immediately after VF and after the ejection of materials from RPV to cavity, water from the hydro-accumulators is automatically injected, and flows into the cavity through the failed RPV. Consequently, about 80 m<sup>3</sup> of water floods the melt in the cavity after the vessel failure, and then slowly boils off on the contact with the (crusted) melt pool, Fig. 6a.

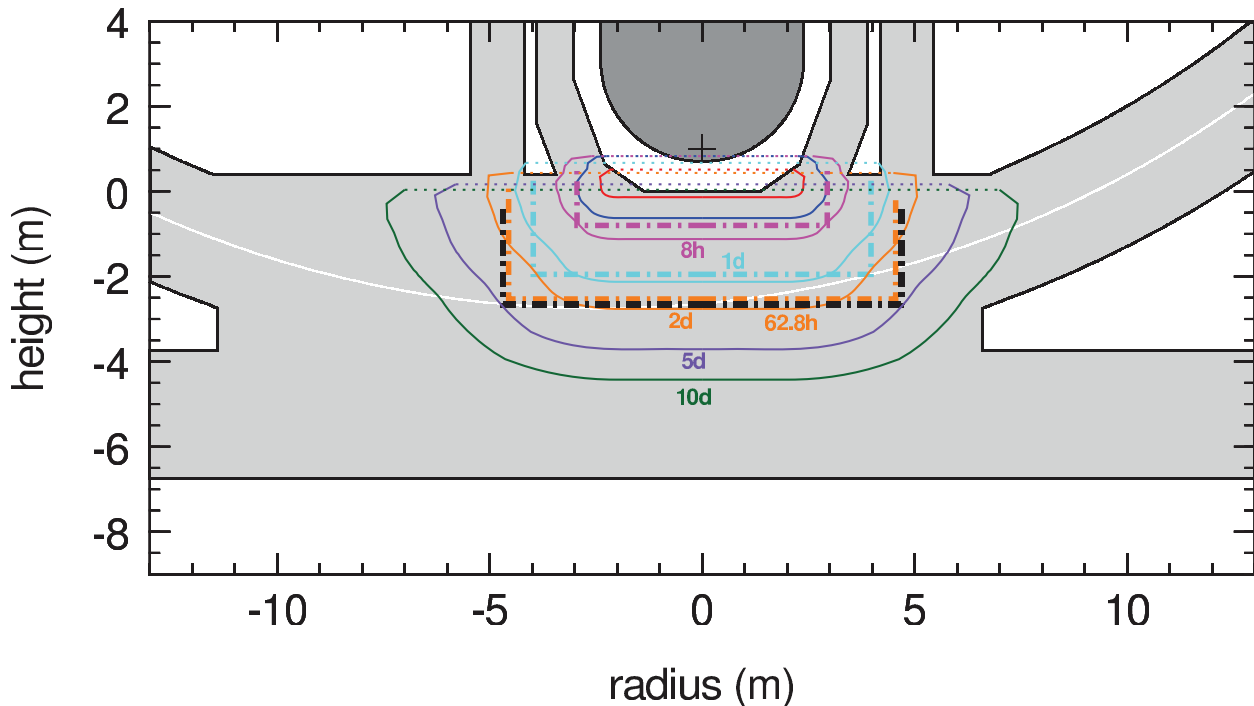


**Figure 2. Cavity ablation predicted by MELCOR (solid lines) and CORQUENCH for the base line scenario**

The MELCOR/CORCON analyses are supplemented by the detailed CORQUENCH analyses. Boundary conditions for the CORQUENCH analyses of the base case SBO sequence reproduce the MELCOR calculations as closely as possible. Most importantly, the decay heat in the cavity and the corresponding mass of reactor materials are used exactly as calculated by MELCOR, as well as the water injection from the accumulators to the cavity after vessel failure, and the boil-off in the cavity. The same modeling options are applied in CORQUENCH as are those used in MELCOR, the most significant being the heat transfer modeling on the melt-concrete interface. In MELCOR, the default approach corresponds to the

situation where a stable gas film forms on the interface by which the heat transfer is determined, the gas\_film model. This is the default both for the basemat surface and for the sideward surfaces. For our KKG simulations, this approach may be justified by the rather high amounts of gases evolving from the concrete of the LCS type (the analyzed concrete contains ~26% wt CaCO<sub>3</sub>).

To be consistent with the MELCOR base case scenario analysis, the gas\_film model was used in the first set of our CORQUENCH simulations. The slag\_film was used in the second set of simulations to study the effect of the two different heat transfer models, together with the effect of the inherent heat conduction calculation which is a part of the slag\_film model in CORQUENCH. In the base line scenario, MELCOR predicts the ejection of materials from the failed RPV in three instances, instead of in one shot, Fig. 3a. Without investigation into the likelihood of such a type of debris ejection we used it exactly the same way also as input for CORQUENCH, Fig. 3b.

The primary results of the base case calculation for the MCCI progression in KKG cavity are shown in Fig. 2. It can be seen that the axial and radial ablation calculated by CORQUENCH is similar to MELCOR up to about 2 days. Here it should be noted that the CORQUENCH calculates a simple cylindrical geometry whereas MELCOR uses a more complex tracking of the ablation profile. MELCOR simulation shows an ongoing ablation which slows down considerably with time. On the other hand, CORQUENCH calculates arrest of the melt at ~62 hours, the ablation stops. This is attributed to conditions where a thick floating upper crust, created when water was atop the melt, is gradually growing even after the overlying water is boiled off and finally encompasses all of the materials in cavity. From the beginning this crust contains a considerable amount of decay heat, Fig. 3b, and its material composition is tracked by CORQUENCH separately from the composition of the melt. In the period after about 10hrs into the accident, the dominant mechanism of the heat removal upwards is radiation. Other similar MCCI analyses by CORQUENCH, for the low pressure variant of the total SBO sequence where there was no water in cavity even for a short time, did not show any melt arrest up to 10 days of the accident progression.

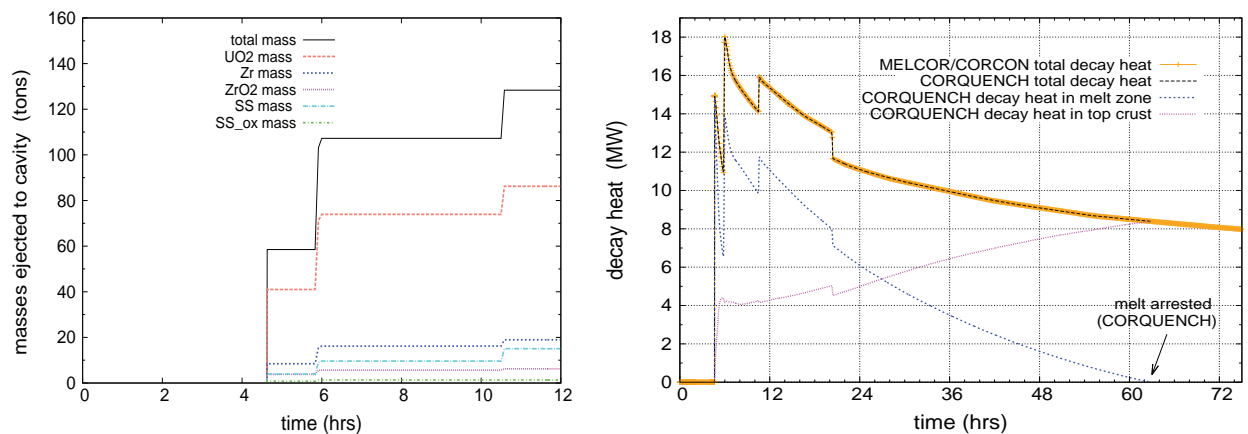


**Figure 3. a) Initial masses of core materials in cavity, b) Total decay heat in cavity by MELCOR and its distribution into the melt and the top crust as calculated with CORQUENCH for the base line scenario**

The energy input, decay heat, and its gradual distribution according to CORQUENCH between the solid part (crust) and the melt zone is shown in Fig. 3b. The corresponding top crust thicknesses in both CORQUENCH and MELCOR calculations are shown in Fig. 4. The axial ablation depth at the time of the melt arrest (marked with the star sign) in CORQUENCH simulations is approximately 270 cm.

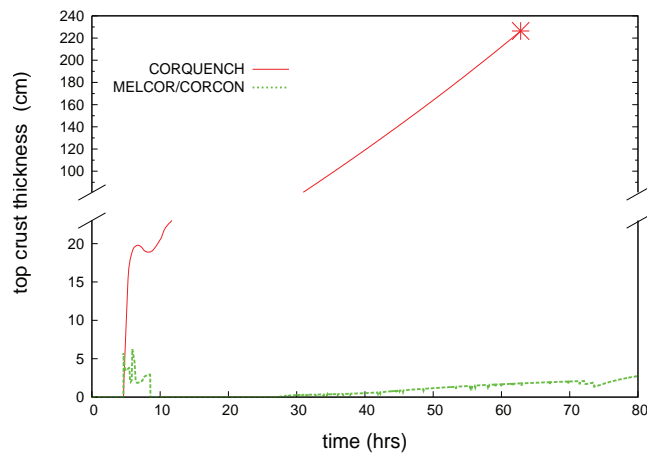


**Figure 4. Thickness of the upper crust calculated with MELCOR and with CORQUENCH**

The distribution of heat loss between the heat going to concrete ablation and the heat removed from the surface of the melt pool is presented in Figs. 5a and 5b for both MELCOR and CORQUENCH (here also with the additional slag\_film CORQUENCH simulation). From the melt surface, the heat may be removed either to the water when the melt is flooded, or by radiation to cavity structures when the cavity is dry.

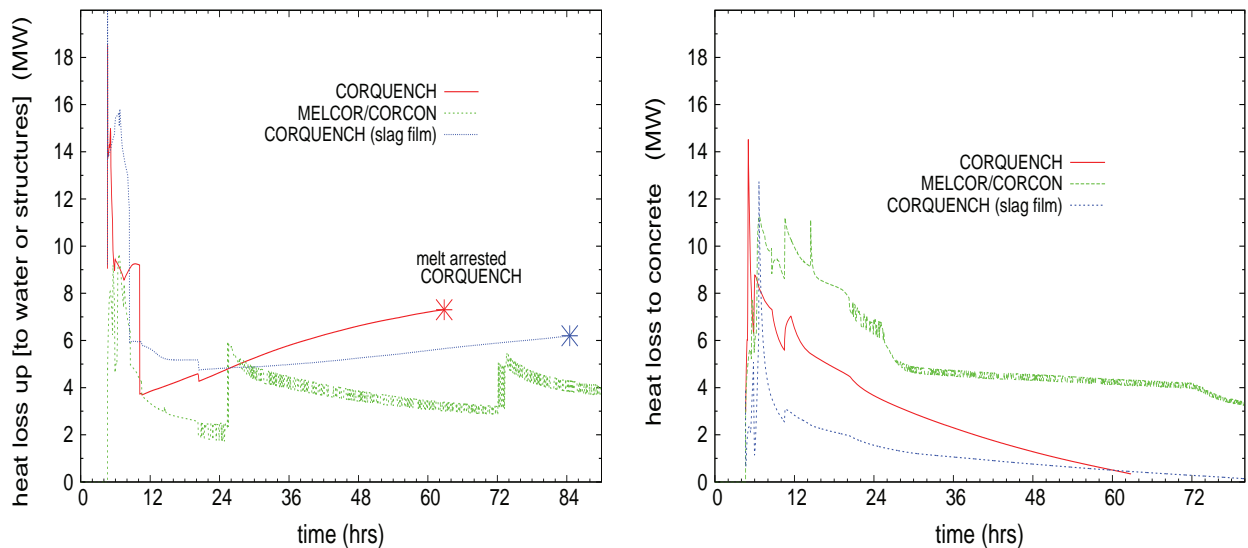


**Figure 5. a) Heat losses upwards from the melt/crust surface, and b) heat loss to concrete as calculated by MELCOR and CORQUENCH**

As long as the melt is flooded (approximately up to 10 hours into the accident), CORQUENCH calculates on average significantly higher removal of the heat upwards than MELCOR, as expected. After the water is lost, the heat removal by radiation from the crusted pool again stays higher with CORQUENCH than with MELCOR. In MELCOR/CORCON modelling, all the decay heat is in the melt, and the thin top crust effectively decreases the heat transfer from the pool, with the majority of decay heat going to ablation, Fig. 5b. Heat going to ablation as calculated by CORQUENCH is decreasing, Fig. 5b, more

steeply than that in MELCOR, and the radiation losses increasing, Fig. 5a (with the increasing upper surface of the melt and approximately constant heat flux upwards of about 100kW/m<sup>2</sup>).

The abrupt changes in the heat loss upwards with the MELCOR simulation at about 25 h and at 73 h, Fig. 5a, are caused by abrupt changes in the calculated upper surface area. This is due to the complex way CORCON is tracking the cavity erosion shape, void fraction in the melt, and the corresponding melt levels and upper surface areas.

#### 4.1. The Effect of the Heat Transfer Modeling

To see the effect of one of the key modeling options, i.e., the treatment of the melt-concrete interface heat transfer, a comparison simulation is performed with CORQUENCH using the slag\_film model option. The results for the base case scenario are presented in Fig. 6. Here as well CORQUENCH predicts melt arrest, though somewhat later than with the gas\_film model option. The axial concrete ablation is much less pronounced in case of the slag\_film model compared to the gas\_film model calculations. The heat conduction losses to concrete calculated with the slag\_film model option -something which is not taken into account in the gas\_film model- could possibly contribute to this (for comparison, there is also shown in Fig. 6b the result of a MELCOR run with the slag\_film model option, non-default option in MELCOR). In this respect the slag\_film model as used in CORQUENCH seems to be a preferable choice over the gas\_film model. The slag\_film model was also chosen for MCCI simulations by MELCOR and CORQUENCH in quite recent analyses of the Fukushima scenarios in Mark I containment [17]. Hence we use it as well in all our sensitivity studies described in chapter 5.

At about 1 day in the base line scenario, calculated heat fluxes across the melt-concrete interface were ~30kW/m<sup>2</sup> with the CORQUENCH slag\_film model, both axially and radially, with  $h_o \sim 70\text{W/K.m}^2$  and  $T_{pool} = 1930\text{K}$ . At the same time, the gas\_film model calculations show heat fluxes of approximately 50kW/m<sup>2</sup> in both CORQUENCH and MELCOR.

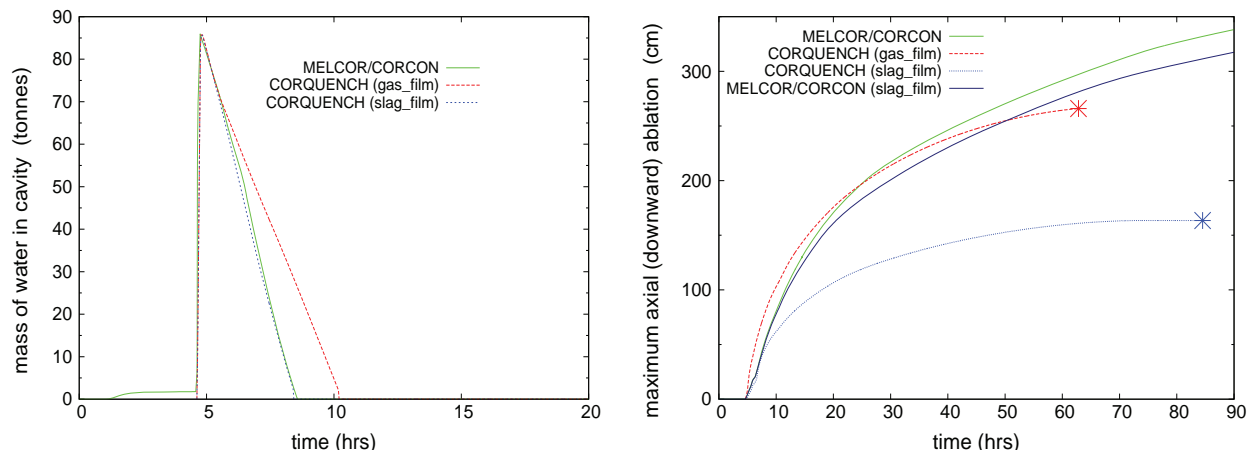


**Figure 6. a) Amount of water in cavity and b) maximum cavity ablation using 2 different heat transfer models in CORQUENCH**

### 5. LONG TERM MCCI COOLABILITY

In this section, CORQUENCH sensitivity analyses are presented for cases where water gets into the cavity at different times after vessel failure, floods the melt, and stays on the melt surface. This represents

accident management measures for the late phase of a severe accident, providing also for a long-term containment heat removal. As described in chapter 3, under these conditions CORQUENCH predictions are considered more reliable than MELCOR due to more detailed modelling of the effect of water on the heat transfer in the crust and on melt surface. Sensitivity simulations are done for a small number of selected parameters and scenarios which are deemed to be the most crucial ones for the KKG analyses. The slag\_film model option is used for all the sensitivity cases.

### 5.1. The Time of Water Addition

The first set of sensitivity calculations concentrates on the time of water addition. Experimental results from the OECD-MCCI projects suggest [18] that early water addition should be much more effective than late addition. To study the effect of the timing with CORQUENCH, three cases are compared, Fig. 7

- base case sequence (slag\_film model employed) where water was present for a relatively short time at the beginning of MCCI
- the same sequence but without water at the beginning of the MCCI, with the addition of water at 5h after vessel failure
- the same sequence, with the addition of water at 25h after vessel failure

The calculated heat losses follow the expected trend, Fig. 7a. High amounts of energy is transferred to water which was present from the beginning of MCCI in the base case sequence, with early boil-off of this water at about 8 h. Following the boil-off of the water, there is much lower heat transfer upwards mostly driven by radiation. There is reduced heat transfer to water in the second sequence due to the later water addition at 5 h after the vessel failure, but the heat transfer continues for a longer time as the isothermal water inventory is maintained in the cavity. Here we assume that containment heat removal is secured. The case with the water addition at 25 h shows the smallest total heat transfer to the water due to the late water injection.

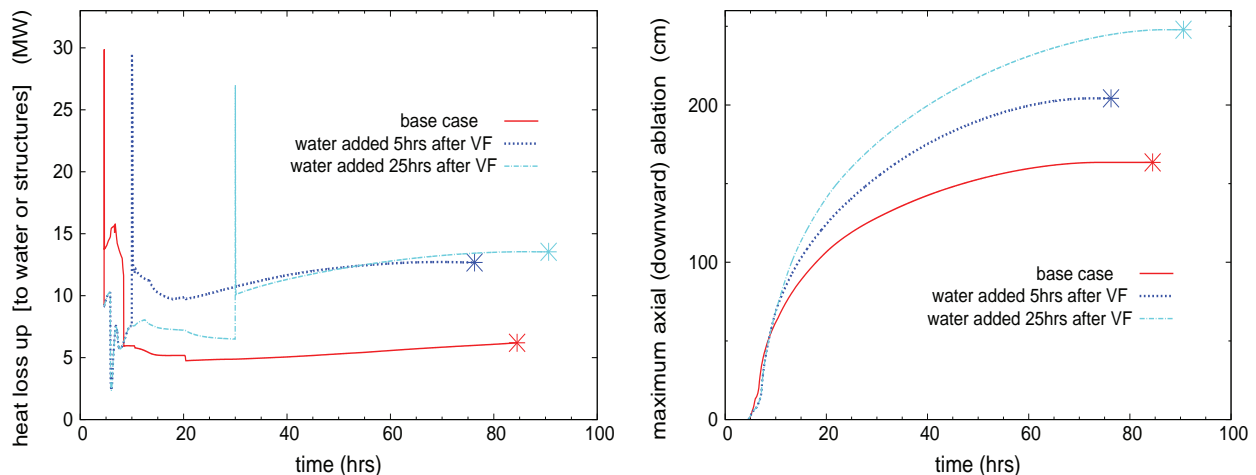


**Figure 7. Sensitivity calculations to study the timing of the water addition; a) heat losses upwards, and b) maximum ablation depth**

After the water addition there is always a short period of bulk cooling, characterized by peak heat fluxes of approximately 1 MW/m<sup>2</sup>. Then the stable crust forms on top of the melt and this high heat removal is not possible any longer. For the sequence with water addition at 5 h after VF there was –immediately after the water addition and up to about 18 h– a considerable contribution to the energy removal from the melt by the eruption mechanism. This was also seen in the other scenario, with the late addition at 25 h after VF, only that the total heat removed by eruptions is much less in that case. In the long term, for both

cases the heat transfer to the water approaches the dryout heat flux limit in a crust of calculated properties (water ingress mechanism; e.g., with the value of ~200 kW/m<sup>2</sup> calculated by the code at about 70 h for the late water addition case).

The energy balances are reflected in the coolability of the melt for the three scenarios, Fig. 7b. For all three cases, CORQUENCH predicts that the melt is arrested, i.e., the MCCI is terminated. The time from the beginning of the sequence to the melt arrest varied from 76 h in the second sequence (water addition at 5 h after the vessel failure) to 91 h in the third sequence (water addition at 25 h after the vessel failure). The ablation depth varies between 1.5 and 2.5 m.

## 5.2. The Effect of Melt Eruption Processes

The second set of sensitivity calculations studies the melt eruption processes which were identified by Robb and Corradini [8] to have the greatest impact on coolability among the MCCI phenomena. Gases evolving from MCCI would vigorously agitate the melt and its surface. The gas generation is rather high for the limestone type concrete used at KKG. The generated gases entrain melt from the melt pool and transport it through holes or cracks in the crust to the top of the crust into the overlying water. The energy associated with the entrained melt is also transported to the surface, and is hence lost from the melt pool. The entrained mass is given by

$$\dot{m}_{me} = (K_e \cdot j_g) \cdot \rho_m \cdot A_m$$

where  $j_g$  is the volumetric flow of gas through the melt (gas superficial velocity),  $\rho_m$  is the density of the melt, and  $A_m$  is the upper surface area. The entrainment coefficient  $K_e$  can be calculated either from a simple correlation based on Ricou-Spalding theory [19] or from very detailed model by Farmer [5]. Both models are included in CORQUENCH. A constant value for  $K_e$  can also be used in the calculation.

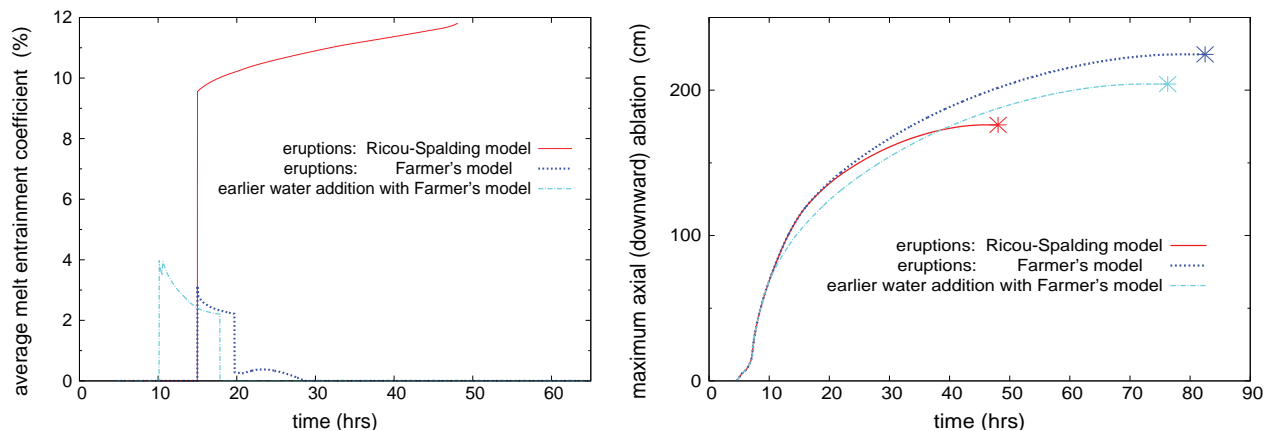


**Figure 8. The effect of melt entrainment model; a) melt entrainment coefficient, and b) the ablation depth, for two different modeling approaches**

The base case sequence calculations in line with the analyses by Robb and Corradini [8] use Farmer's model for evaluation of the energy losses by eruptions. Water is added on top of the melt at 15 h after the accident initiation. To examine the effect of using the alternative formulation, CORQUENCH simulation with the eruption model based on Ricou-Spalding theory was also carried out. In the third simulation, using again the Farmer's model, earlier water addition was examined, at 10 h instead of 15 h after the accident initiation. The calculated entrainment of the melt is much higher with the Ricou-Spalding model, Fig. 8a, representing more than 10% of the entraining gas volumetric flow, persisting for a very

long time. The Farmer’s model yields entrainment up to 4% at maximum and the eruptions are active only for a limited period of time. With this model a minimum, threshold superficial gas velocity is calculated in the code which is required to maintain active vent holes on the crust surface (the modeling addresses the thermal hydraulic flow, pressure drop, and freezing process involved with melt ejections through a crust that is permeable to both gas and water flows [5]). The end of the active eruption periods in the two simulations with the Farmer’s model, Fig. 8a, corresponds to the time when the actual calculated gas velocity, volumetric flow rate of gas, drops below this threshold (minimum) velocity. It happened at ~17 h 50 min for the calculated gas velocity of about 2 cm/s in the first simulation (earlier water addition, light blue curve) and at ~28 h 40 min for the gas velocity of 1.2 cm/s in the other simulation (dark blue curve). With the simple correlation based on Ricou-Spalding there is no dependence on the gas velocity or on the density of the active vent holes in the permeable crust so the model predicts continuous entrainment of the melt.

The impact of the entrainment modeling on erosion depth and on coolability can be seen in Fig. 8b. As expected, the high entrainment coefficient calculated with the correlation based on Ricou-Spalding theory gives much earlier arrest of the melt than the calculation with the Farmer’s model, 48 h and 84.5 h, respectively. According to the calculated average values of  $K_e$  in this work, the Farmer’s model is deemed to be more reliable.

### 5.3. Anchored Crust

Our last sensitivity simulations concentrate on the possibility that the top crust may become anchored to the sidewalls of the cavity and form a stable, solid “bridge” above the melt. This situation has been observed in the medium scale tests of the MACE experimental program (ca. 1m x 1m rectangular test concrete cavity and up to 2 metric tons of core melt mass). In such a case the melt which is eroding the concrete and receding downwards, may detach from the stable crust which has the cooling water on its surface. If the crust remains stable and anchored to the sidewalls the melt would be isolated from the water on the crust surface and, consequently, the water would not be able to cool the melt. It has been postulated that in a reactor scale (~6 m diameter cavities), the anchored crust would break due to its own weight. With water on its surface, the mass of the water would increase the probability of breaking the crust [20]. Recent OECD-MCCI projects have provided data on the strengths of prototypical crusts [18] which support this notion.

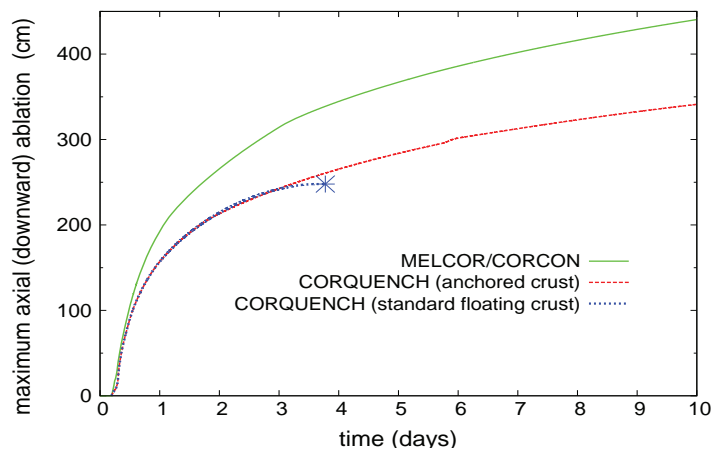


**Figure 9. Ablation depth for the anchored crust case with CORQUENCH, and comparison with MELCOR**

The CORQUENCH calculation for the KKG cavity was carried out with the “anchored crust” option switched on, and it is presented in Fig. 9. Compared to the standard “floating crust” calculation and the MELCOR base line calculation it is seen that in the case of the anchored crust the MCCI is not arrested within the first ten days of the accident, as is the case for the floating crust scenario. Compared to the MELCOR simulations, the anchored crust case shows smaller ablation depth. Both CORQUENCH calculations here represent the most unfavourable case with the water getting into the cavity only after 30 h, i.e. 25 h after vessel failure.

In an attempt to estimate the time of basemat melt-through predicted by CORQUENCH under the anchored crust conditions, the simulation was continued for 20 days of the accident. The calculated downward ablation at this time was approximately 4 m and the predicted rate of ablation was some millimeters per hour. Based on this, additionally more than 40 days would be required to reach the basemat melt-through if the rate of ablation would stay constant.

## 6. SUMMARY

MELCOR/CORCON and CORQUENCH analyses were performed for several postulated long-term SBO scenarios in a KONVOI PWR to study the cavity response to extended MCCI. Main interest was in the evaluation of the long-term basemat concrete erosion under different conditions in the cavity during the accident, using homogeneous melt configuration. Also, the possible arrest of the melt in the cavity, i.e., terminating the MCCI progression, was studied with water addition to cavity as a part of the late-phase AM. The effect of different modeling assumptions on the simulation results was investigated by several sensitivity cases, including the effect of the heat transfer modeling on the melt-concrete interface.

This type of KONVOI containment appears to be relatively resistant to challenges by the late-phase accident progression. As shown by the analyses, the thick cavity basemat, about 6.5 m, guarantees a very long time to axial (downward) melt-through. All calculations executed with CORQUENCH with water atop the melt and without the very unlikely anchored crust scenario showed arresting of the melt long before the basement was endangered. For all cases with the late water addition the favorable predictions by CORQUENCH are more reliable than MELCOR predictions due to the missing coolability models in MELCOR. The radial ablation was not a focus of this study, but it does not seem to pose a challenge to the integrity of this containment.

For the base line SBO scenario, where water flooded the melt only for a short period of time, CORQUENCH predicts melt arrest at approximately 63 h with less than a half of the total basemat thickness eroded. With the slag\_film option and the concrete dry-out modeling -as a preferred choice of the heat transfer modeling in CORQUENCH- the calculated concrete ablation, both axial and radial, was substantially less pronounced with CORQUENCH than with MELCOR. Thus, apart from the coolability models, it could be useful for MELCOR/CORCON to include as an option also the heat conduction modeling (concrete dry-out) in a similar way as it is done in CORQUENCH.

## ACKNOWLEDGMENTS

The authors gratefully acknowledge the financial support and technical input from Kernkraftwerk Gösgen -Däniken AG, Kernkraftwerk Gösgen (KKG), on whose behalf the present study was performed.

## REFERENCES

1. M.T. Farmer, D.J. Kilsdonk, R.W Aeschlimann, “Corium Coolability under Ex-Vessel Accident Conditions for LWR”, *Nuclear Engineering and Technology*, **41**, pp. 575-602 (2009)

2. C.Journeau et al., “Contributions of the VULCANO Experimental Programme to the Understanding of MCCI Phenomena”, *Nuclear Engineering and Technology*, **44**, pp. 261-272 (2012)
3. J.J. Foit, “Overview and history of core concrete interaction issues”, *Proc. of OECD/NEA MCCI Seminar*; Cadarache, France (2007)
4. R.O. Gaunt et al., MELCOR Computer Code Manuals, Version 1.8.6, NUREG/CR6191 (2005)
5. M.T. Farmer, “The CORQUENCH Code for Modeling of Ex-Vessel Corium Coolability under Top Flooding Conditions, Code Manual – Version 3.03”, OECD/MCCI-2010-TR03 (2010)
6. D.R. Bradley et al., “CORCON-MOD3: An Integrated Computer Model for Analysis of Molten Core-Concrete Interactions”, User’s Manual, NUREG-CR-5843, SAND92-0167 (1993)
7. K.R. Robb, M.L. Corradini, “MCCI Simulation Comparison between MELCOR and CORQUENCH”, *Proceedings NURETH-14*, Toronto, Ontario, Canada (2011)
8. K.R. Robb, M.L. Corradini, 2010, “Ex-Vessel Core Melt Coolability Simulation with CORQUENCH and MELCOR”, OECD-MCCI-2 Seminar, Cadarache, France (2010)
9. T.G. Theofanous, C. Liu, S. Additon, S. Angelini, O. Kymäläinen, T. Salmassi, “In-vessel coolability and retention of a core melt”, *Nucl.Eng.Des.* **169**, pp. 1-48 (1997)
10. S.S. Kutateladze and I.G. Malenkov, “Boiling and Bubbling Heat Transfer under the Conditions of Free and Forced Convection”, *6<sup>th</sup> Int. Heat Transfer Conference*, Toronto (1978)
11. D.R. Bradley, “Modeling of Heat Transfer between Core Debris and Concrete”, *ANS Proceedings of the 1998 National Heat Transfer Conference*, Houston, TX (1988)
12. V.K. Dhir, J.N. Castle, I. Catton, "Role of Taylor Instability on Sublimation of a Horizontal Slab of Dry Ice", *J.Heat Transfer*, 99, p.411 (1977)
13. M. Epstein, “Heat Conduction in the UO<sub>2</sub>-Cladding Composite Body with Simultaneous Solidification and Melting”, *Nuclear Science and Engineering*, **51** (1973)
14. M.T. Farmer, “Status of Modeling Activities”, *6<sup>th</sup> OECD-MCCI2 Program Review Meeting*, Argonne National Laboratory, April 20-21 (2009)
15. J.M. Seiler, H. Combeau, “Transient interface temperature on a vertical surface in multi-component solid-liquid systems with volume heating”, *Nucl.Eng.Des.* **278**, pp. 199-208 (2014)
16. J.M. Bonnet, C. Spengler, T. Sevón, A. Rýdl, “Review of 10 years of molten corium concrete interaction R&D –potential applications for containment integrity”, Eurosafe Forum 2010 -Innovation in Nuclear Safety and Security, Cologne, Germany (2010)
17. K.R. Robb, M.W. Francis and M.T. Farmer, “Ex-Vessel Core Melt Modeling Comparison between MELTSPREAD-CORQUENCH and MELCOR 2.1”, ORNL/TM-2014/1 (2014)
18. S. Lomperski, M.T. Farmer, “Measurements of the Mechanical Strength of Corium Crusts”, *Proc. ICAPP’08*, Anaheim, CA (2008)
19. F.P. Ricou, D.B. Spalding, “Measurements of entrainment by axisymmetrical turbulent jets”, *Journal of Fluid Mechanics* **Vol 11**(1), pp. 21-32 (1961)
20. K.R. Robb, M.L. Corradini, “Ex-Vessel Corium Coolability Sensitivity Study with the CORQUENCH code”, *Proceedings NURETH-13*, Kanazawa, Japan, September 27 (2009)
21. A. Tenaud, C. Caroli, “MCCI analyses in support of the Probabilistic Safety Assessment level 2 for the French 900 MWe PWR”, OECD-MCCI Seminar, Cadarache, France (2007)